

Active and Reactive Power Control of Battery Energy Storage Systems in Weak Grids

Luis Rouco and Lukas Sigrist
Universidad Pontificia Comillas
Alberto Aguilera, 23
28015 Madrid, Spain

Abstract

This paper proposes outer loop active and reactive power controllers to ensure battery energy storage system (BESS) performance when connected to a network that exhibits low short circuit ratio. Inner loops control the BESS current components. The interface of BESSs with the grid is based on voltage source converters of STATCOM type which allow BESS providing not only active power control but also reactive power/voltage control. A meaningful design approach of both inner and outer loop controls is presented. Time domain simulation results show the problems encountered and the performance of the proposed control scheme.

Introduction

Recent developments in Li-Ion and NaS battery technologies are making battery energy storage systems (BESSs) feasible for a number of power system applications [1]. Weak grids exhibit specific features that can make the application of BESSs more profitable than in strong grids. Weak grids are characterized by large voltage and frequency excursions due to low short circuit ratio and to low mechanical inertia, respectively [2]. For instance, economic benefits of providing frequency primary regulation reserve with BESSs in small isolated systems have been determined in [3].

A meaningful application of BESSs in weak grids with low circuit ratio consists of connecting the BESS to the MV bus bar of a HV/MV transformer station. The BESS can alleviate the congestion of the HV line when supplying the peak load of the substation. The congestion of the HV line occurs when the load of the transformer station is higher than the HV line rate rating. It may be due to the fact that other HV line that feeds the transformer station, is temporarily out of service. The usual mitigation approach of this type of congestion consists in installing an emergency generator in the

substation and connecting it to the MV bus bar like the BESS.

The interface of BESSs with the grid is nowadays based on voltage source converters of STATCOM type. Hence, BESS can provide not only active power control but also reactive power/voltage control ([4]-[6]). Assuming that the battery voltage is constant despite load variation (it is usually achieved by a DC/DC converter between the battery itself and the voltage source converter), the component of the current in the d-axis of a reference frame rotating at synchronous speed and solid to the terminal voltage controls the active power, whereas the component of the current in the q-axis in the same frame controls the reactive power. If the BESS is connected to network that exhibits a high short circuit ratio (strong network), this control scheme works satisfactorily. However, if the BESS is connected to a weak network, the d-axis and q-axis controls become coupled.

This paper proposes outer loop active and reactive power controllers to ensure BESS performance when connected to a network that exhibits low short circuit ratio. A meaningful design approach of both inner and outer loop controls is presented. Time domain simulation results show the problems encountered and the performance of the proposed control scheme.

BESS Connected to an Infinite Grid

A BESS consists of a battery connected to the grid through a voltage source converter and a filter as shown Fig. 1.

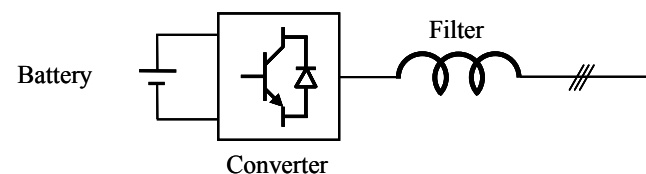


Fig. 1: Battery Energy Storage System connected to an infinite grid.

Converter Model

By assuming that the converter is represented as an ideal voltage source, of which components can be independently controlled, the equivalent circuit of the converter and the connecting filter is shown in Fig. 2. The complex equations in a synchronous rotating reference frame that describe the equivalent circuit of Fig. 2. are:

$$\mathbf{v} = \mathbf{R}_a \mathbf{i}_a + \frac{1}{\omega_0} \frac{d\boldsymbol{\Psi}_a}{dt} + j\omega_s \boldsymbol{\Psi}_a + \mathbf{v}_a \quad (1)$$

$$\boldsymbol{\Psi}_a = \mathbf{L}_a \mathbf{i}_a \quad (2)$$

where:

ω_s is the speed of the synchronous reference frame in pu and

ω_0 is the speed base in rad/s.

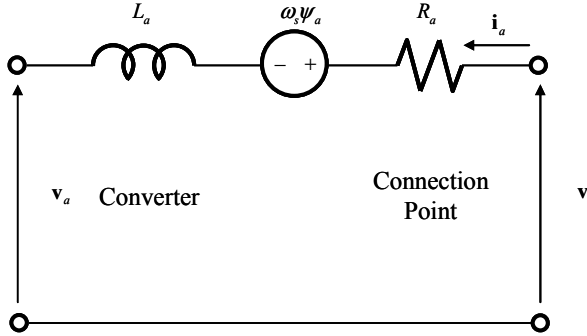


Fig. 2: Equivalent circuit of the converter.

If equations (1) and (2) are rewritten in real form, they become:

$$\begin{aligned} v_d &= R_a i_{ad} + \frac{1}{\omega_0} L_a \frac{di_{ad}}{dt} - \omega_s L_a i_{aq} + v_{ad} \\ v_q &= R_a i_{aq} + \frac{1}{\omega_0} L_a \frac{di_{aq}}{dt} + \omega_s L_a i_{ad} + v_{aq} \end{aligned} \quad (3)$$

Control of Converter Current Components

The dynamics of the current components can be decoupled if two auxiliary variables (v'_{ad} y v'_{aq}) are defined:

$$\begin{aligned} v'_{ad} &= v_d + \omega_s L_a i_{aq} - v_{ad} = R_a i_{ad} + \frac{1}{\omega_0} L_a \frac{di_{ad}}{dt} \\ v'_{aq} &= v_q - \omega_s L_a i_{ad} = R_a i_{aq} + \frac{1}{\omega_0} L_a \frac{di_{aq}}{dt} \end{aligned} \quad (4)$$

Hence, the decoupled current component dynamics can be represented by the following first order systems:

$$\frac{i_{ad}(s)}{v'_{ad}(s)} = \frac{\frac{1}{R_a}}{1 + \frac{1}{\omega_0} \frac{L_a}{R_a} s}$$

$$\frac{i_{aq}(s)}{v'_{aq}(s)} = \frac{\frac{1}{R_a}}{1 + \frac{1}{\omega_0} \frac{L_a}{R_a} s}$$

The decoupled current components are controlled by PI controllers as shown in Fig. 3.

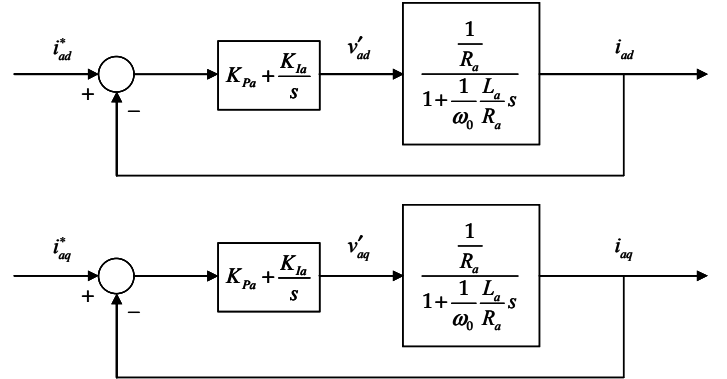


Fig. 3: Current component control loops.

The PI controllers are designed in such a way that the equivalent second order system exhibits the selected undamped natural frequency (typical values are 25 rad/s and damping 70%). Depending on the converter's overload capability, a faster response through a larger undamped natural frequency might be necessary. The transfer function of a feedback control system, where the plant is a first order system $K/(1+sT)$ and the regulator is a PI controller $(K_p + K_I/s)$, is:

$$\frac{y(s)}{u(s)} = \frac{(K_p s + K_I) \frac{K}{T}}{s^2 + \left(\frac{1 + K_p K}{T} \right) s + \frac{K_I K}{T}} = \frac{(K_p s + K_I) \frac{K}{T}}{s^2 + 2\zeta\omega_n s + \omega_n^2}$$

Hence, the parameters of the PI regulator can be obtained as:

$$K_p = 2\zeta\omega_n T$$

$$K_i = \omega_n^2 T$$

The actual values of the voltage components of the converter can be obtained from (4) as:

$$v_{aq} = v_q - \omega_s L_a i_{ad} - v'_{aq}$$

$$v_{ad} = v_d + \omega_s L_a i_{aq} - v'_{ad}$$

Hence, the block diagrams of the decoupled current component controllers are displayed in Fig. 4.

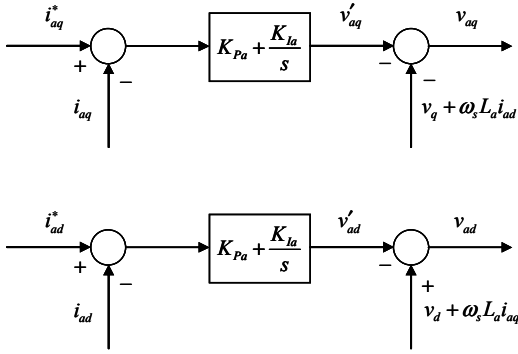


Fig. 4: Current component controllers.

The equations of the decoupled current component controllers of Fig. 4 can be written in state space form as:

$$\begin{aligned} \dot{x}_{a1} &= K_{Ia} (i_{aq}^* - i_{aq}) \\ v'_{aq} &= x_{a1} + K_{Pa} (i_{aq}^* - i_{aq}) \\ v_{aq} &= v_q - \omega_s L_a i_{ad} - v'_{aq} \\ \dot{x}_{a2} &= K_{Ia} (i_{ad}^* - i_{ad}) \\ v'_{ad} &= x_{a2} + K_{Pa} (i_{ad}^* - i_{ad}) \\ v_{ad} &= v_d + \omega_s L_a i_{aq} - v'_{ad} \end{aligned} \quad (5)$$

BESS Model

The equations of the converter (4) and current controllers (5) can be written as a set of differential and algebraic equations:

$$\begin{aligned} \dot{\mathbf{x}} &= \mathbf{f}(\mathbf{x}, \mathbf{z}, \mathbf{u}) \\ \mathbf{0} &= \mathbf{g}(\mathbf{x}, \mathbf{z}, \mathbf{u}) \end{aligned} \quad (6)$$

where:

\mathbf{x} is the vector of state variables
 \mathbf{z} is the vector of algebraic variables
 \mathbf{u} is the vector of input variables

$$\mathbf{x}^T = [\psi_{ad} \ \psi_{aq} \ x_{a1} \ x_{a2}]$$

$$\mathbf{z}^T = [i_{ad} \ i_{aq} \ v_{ad} \ v_{aq} \ v'_{ad} \ v'_{aq}]$$

$$\mathbf{u}^T = [v_d \ v_q \ i_{ad}^* \ i_{aq}^*]$$

Simulation of a BESS Model

Let us assume that the parameters of the connection filter BESS are:

$$R_a = 0.008 pu \quad L_a = 0.08 pu$$

Let us also consider that BESS is working at the following operating point:

$$v_{d0} = 1 pu \quad v_{q0} = 0 pu \quad i_{ad0} = -0.8 pu \quad i_{aq0} = 0 pu$$

which means that the voltage of the connection point is the nominal one and it supplies active current and no reactive current. A -0.6 pu step at the reactive current reference is applied (i.e., the current will not exceed the nominal rating in steady state).

Time variation of the d- and q-axis current components is shown in Fig. 5. The desired value of the q-axis current component is achieved, whereas the d-axis current component remains constant due to the proper action of the current controllers. Note also that the current only slightly exceeds the nominal rating during the transient (about 2% compared to the usual overload capability of 110% of nominal rating). It must be noted that as the voltage of the connection point is assumed to be constant, the active and reactive powers are equal to the d- and q-axis current components respectively.

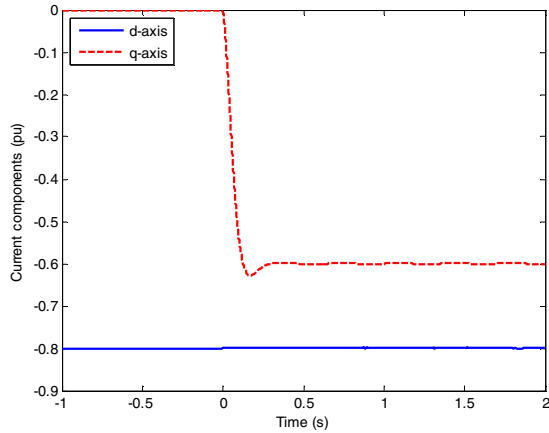


Fig. 5: Response to a step of q-axis current component: d- and q-axis current components.

BESS Connected to a Weak Grid

A meaningful application of BESSs in weak grids with low circuit ratio is depicted in Fig. 6. A BESS connected

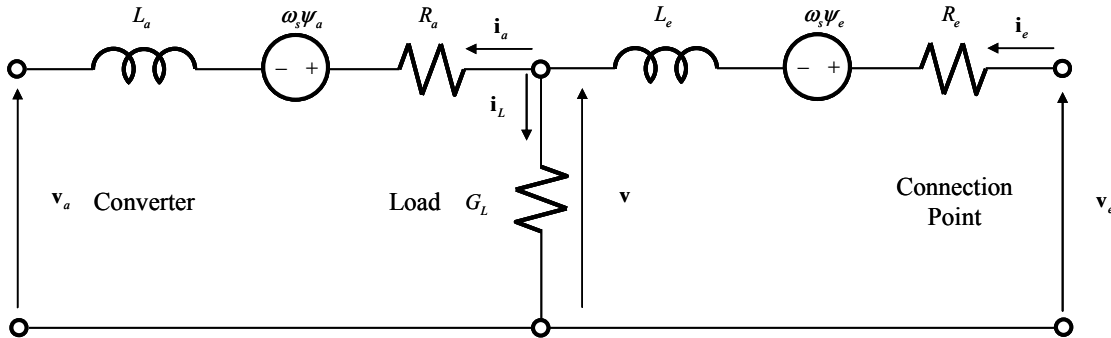


Fig. 7: Response to a step of reactive power: d- and q-axis current components and active and reactive powers.

Model of BESS Connected to a Weak Grid

The equivalent circuit of a BESS connected to a weak grid is shown Fig. 7. It is built by adding to the equivalent circuit of the converter and the connection filter a pure resistive load at the BESS connection point as well as a connection impedance to the infinite grid that represents the impedance of the HV/MV transformer and the HV line.

The equations of the connection impedance and the load written in real form with respect to a frame rotating at synchronous speed are:

to the MV bus bar of a HV/MV transformer station can alleviate the congestion of the HV line when supplying the peak load of the substation. The congestion of the HV line occurs when the load of the transformer station is higher than the HV line rating. It may be due to the fact that another HV line that feeds the transformer station is temporarily out of service. The usual mitigation approach of this type of congestion consists in installing an emergency generator in the substation and connecting it to the MV bus bar like the BESS.

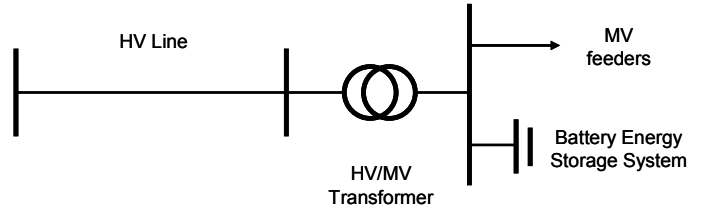


Fig. 6: Application of BESS for alleviating a congested line.

$$\begin{aligned}
 v_{ed} &= R_e i_{ed} + \frac{1}{\omega_0} L_e \frac{di_{ed}}{dt} - \omega_s L_e i_{eq} + v_d \\
 v_{eq} &= R_e i_{eq} + \frac{1}{\omega_0} L_e \frac{di_{eq}}{dt} + \omega_s L_e i_{ed} + v_q \\
 i_{ed} &= i_{Ld} + i_{ad} \\
 i_{eq} &= i_{Lq} + i_{aq} \\
 i_{Ld} &= G_L v_d \\
 i_{Lq} &= G_L v_q
 \end{aligned} \tag{7}$$

The equations of the current controllers expressed with respect to the BESS terminal voltage are:

$$\begin{aligned}
\hat{\mathbf{i}}_a &= \mathbf{i}_a e^{-j\angle v} \\
\hat{i}_{ad} &= \text{Re}\{\hat{\mathbf{i}}_a\} \\
\hat{i}_{aq} &= \text{Im}\{\hat{\mathbf{i}}_a\} \\
\dot{x}_{a1} &= K_{la} (i_{aq}^* - \hat{i}_{aq}) \\
v'_{aq} &= x_{a1} + K_{pa} (i_{aq}^* - \hat{i}_{aq}) \\
\hat{v}_{aq} &= -\omega_s L_a \dot{i}_{ad} - v'_{aq} \\
\dot{x}_{a2} &= K_{la} (i_{ad}^* - \hat{i}_{ad}) \\
v'_{ad} &= x_{a2} + K_{pa} (i_{ad}^* - \hat{i}_{ad}) \\
\hat{v}_{ad} &= v + \omega_s L_a \dot{i}_{aq} - v'_{ad} \\
\mathbf{v}_a &= (\hat{v}_{ad} + j\hat{v}_{aq}) e^{j\angle v} \\
v_{ad} &= \text{Re}\{\mathbf{v}_a\} \\
v_{aq} &= \text{Im}\{\mathbf{v}_a\}
\end{aligned} \tag{8}$$

The equations of the converter (4), the connection impedance and the load (7) and the current controllers (8) can be written as a set of differential and algebraic equations (6) where:

$$\begin{aligned}
\mathbf{x}^T &= [\psi_{ad} \ \psi_{aq} \ x_{a1} \ x_{a2} \ \psi_{ed} \ \psi_{eq}] \\
\mathbf{z}^T &= [i_{ad} \ i_{aq} \ \hat{i}_{ad} \ \hat{i}_{aq} \ v_{ad} \ v_{aq} \ \hat{v}'_{ad} \ \hat{v}'_{aq}] \\
\mathbf{u}^T &= [v_d \ v_q \ i_{ad}^* \ i_{aq}^*]
\end{aligned}$$

Simulation of a BESS Connected to a Weak Grid

Let us assume that the parameters of the connection impedance and the load are:

$$R_e = 0.08 \text{ pu} \quad L_e = 0.8 \text{ pu} \quad G_L = 1.6 \text{ pu}$$

A -0.6 pu step at the reactive current reference is applied again. Fig. 8 shows the time variation of the current components. The q-axis current component achieves the desired value whereas the d-axis current component remains constant.

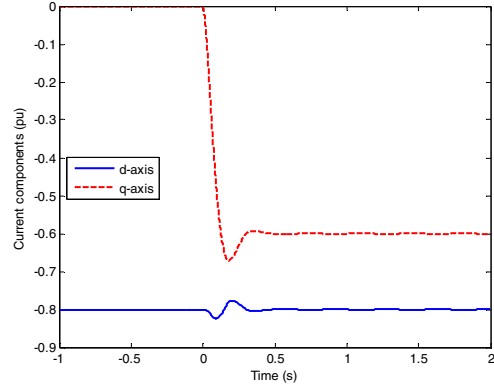


Fig. 8: Response to a step of q-axis current component: d- and q-axis current components.

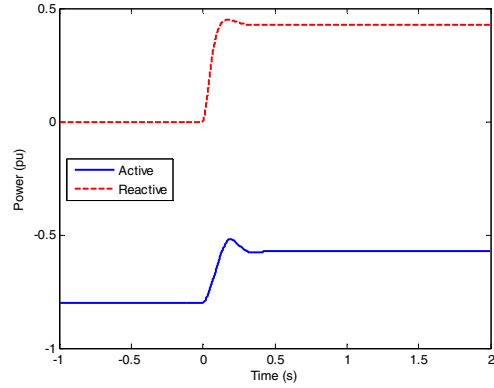


Fig. 9: Response to a step of q-axis current component: active and reactive powers.

Time variation of the active and reactive powers is shown in Fig. 9. As the BESS terminal voltage exhibits large excursions (see Fig. 10) due to the low short circuit ratio, controlling the current components does not mean that the active and reactive powers are properly controlled.

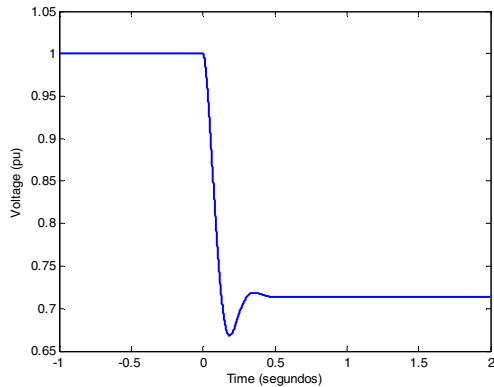


Fig. 10: Response to a step of q-axis current component: BESS terminal voltage.

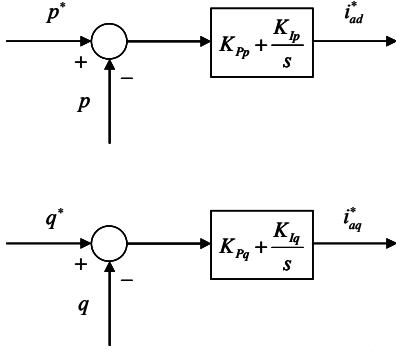


Fig. 11: Active and reactive power controllers.

Active and Reactive Power Controllers

The problems encountered when connecting a BESS to a weak grid can be addressed by adding active end reactive power controller as shown in Fig. 11. The active power controller commands the reference of the d-axis current component whereas the reactive power controller commands the reference of the q-axis current component.

The active and reactive power controllers are designed considering the control loop depicted in Fig. 12. They assume that the d-axis component of the BESS terminal voltage is constant and that $v_q i_{aq}$ and $v_q i_{ad}$ terms are disturbances.

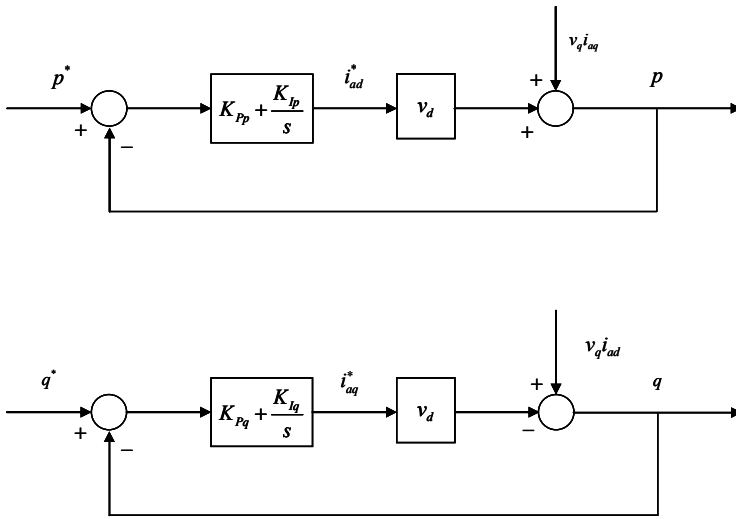


Fig. 12: Active and reactive power control loops.

The PI controllers are designed in such a way that the equivalent first order system is a lag filter exhibits the selected maximum lag frequency and filter ratio (typical values are 2.5 rad/s and 2 respectively). This way the power controller responses are much slower than the current controller responses and interference is prevented. The transfer function of a feedback control system, where the plant is a static gain K and the regulator is a PI controller $(K_p + K_i/s)$, is:

$$\frac{y(s)}{u(s)} = \frac{\frac{K_p}{K_i} s + 1}{\frac{(1 + K_p K)}{K_i K} s + 1} = \frac{T_1 s + 1}{T_2 s + 1}$$

By taking into consideration the relationship between the maximum lag frequency and the filtering ratio with the time constants of the lag filter:

$$\omega = \frac{1}{\sqrt{T_1 T_2}}$$

$$\alpha = \frac{T_2}{T_1}$$

the parameters of the PI regulator can be determined as:

$$K_p = \frac{1}{K \left(\frac{T_2}{T_1} - 1 \right)}$$

$$K_i = \frac{K_p}{T_1}$$

Simulation of a BESS Connected to a Weak Grid with Active and Reactive Power Controllers

A -0.6 pu step at the reactive power reference is applied in this case. Fig. 13 shows the time variation of the active and reactive powers. The reactive power achieves the desired value whereas the active power remains constant. Fig. 14 displays the time variation of the d- and q-axis current components. Both current components change to attain the desired values of the active and reactive powers. Fig. 15 shows the BESS terminal voltage. As the BESS is supplying reactive power to the grid, the terminal voltage increases.

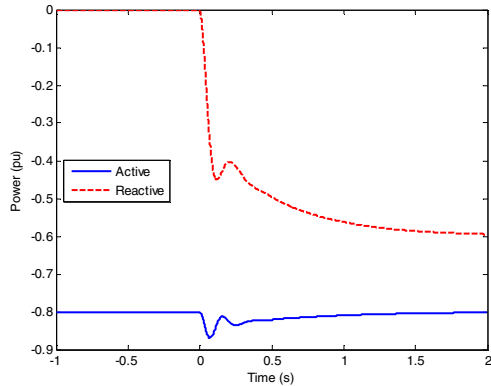


Fig. 13: Response to a step of q-axis current component: active and reactive powers.

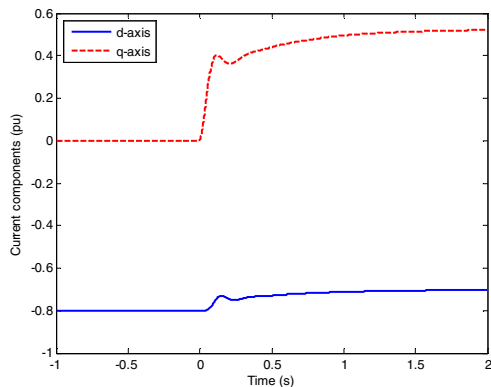


Fig. 14: Response to a step of q-axis current component: d- and q-axis current components.

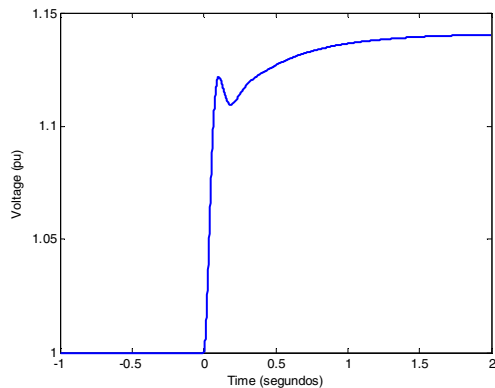


Fig. 15: Response to a step of q-axis current component: BESS terminal voltage.

Conclusions

This paper has studied the design and performance of the control loops of a BESS connected to the grid through a STATCOM type power electronic converter. Precisely, the paper has shown that active and reactive power outer control loops, in addition to inner control loops of current components, are needed when the BESS is connected to a weak grid characterized by a low short circuit ratio.

Acknowledgements

The ideas of this paper have been developed within the research environment of the STORE project sponsored by Endesa. We are grateful for this environment and for the support of a number of Endesa engineers. Special thanks are due to Mr. A. Barrado, Mr. P. Fontela and Mr. J. Magriñá.

References

- [1] A. Nourai, "Large-Scale Electricity Storage Technologies for Energy Management", 2002 IEEE Power Engineering Society Summer Meeting, Volume 1, pp. 310 – 315.
- [2] IEEE, "IEEE Guide for Planning DC Links Terminating at AC Locations Having Low Short-Circuit Capacities", IEEE Std. 1204-1997, 1997.
- [3] E. Lobato, L. Rouco, L. Sigríst, M. Cruz, P. Fontela, J. Magriñá, E. Moreda, "Economic assessment of providing primary reserve service with energy storage systems in isolated systems", 44 Cigré Session, Paris, France, 27-31 August 2012, paper No. C6-307.
- [4] C. Banos, M. Aten, P. Cartwright, T. C. Green, "Benefits and control of STATCOM with energy storage in wind power generation", Proceedings of the 8th IEE International Conference on AC and DC Power Transmission, 2006, pp. 230 – 235.
- [5] B. Gudimetla, S. Teleke, J. Castaneda, "Application of Energy Storage and STATCOM for grid quality issues", 2011 IEEE Power and Energy Society General Meeting, San Diego, CA, USA. July 22-27, 2012.
- [6] J. Castaneda, J. Enslin, D. Elizondo, N. Abed, S. Teleke, "Application of STATCOM with energy storage for wind farm integration", 2010 IEEE PES, Transmission and Distribution Conference and Exposition, New Orleans, LA, USA, April 19 – 22, 2010.